Thermal and Mechanical Behavior of Unsaturated Polyester [Derived from Poly(ethylene terephthalate) Waste] and Montmorillonite-Filled Nanocomposites Synthesized by *In Situ* Polymerization

Sunain Katoch,[1] P. P. Kundu[1,2]

[1]*Department of Chemical Technology, Sant Longowal Institute of Engineering & Technology, Sangrur, Punjab 148106, India*
[2]*Department of Polymer Science & Technology, University of Calcutta, 92, A. P. C. Road, Kolkata 700009, India*

Received 11 May 2010; accepted 21 December 2010
DOI 10.1002/app.34042
Published online 29 June 2011 in Wiley Online Library (wileyonlinelibrary.com).

ABSTRACT: Postconsumer poly(ethylene terephthalate) waste bottles were glycolyzed as precursors of unsaturated polyester resin (UPR) and their montmorillonite (MMT)-filled nanocomposites. The glycolysis product (hydroxyl-terminated oligomers) was converted into UPR with various acid contents. These resins were miscible with styrene and could be cured with peroxide initiators to produce thermosetting unsaturated polyester (UP). Nanocomposites composed of UP matrix and organically modified clay were prepared by *in situ* polymerization. These were characterized for thermal and dynamic mechanical properties. Transmission electron microscopy was also used to study the morphology at different length scales and showed the nanocomposites to be compromised of a random dispersion of intercalated/exfoliated aggregates throughout the matrix. With an increase in unsaturated acid content (for a fixed content of clay), the value of storage modulus varied from 2737 to 4423 MPa. The glass-transition temperatures of these nanocomposites ranged from 54 to 78°C, and the crosslink density varied from 3.70×10^5 to 5.72×10^5 mol/m^3. The X-ray diffraction (XRD) of modified MMT exhibited a peak that vanished completely in the polymer nanocomposites. Thus, the XRD results apparently indicated a distortion of the platy layers of nanofiller in the UP nanocomposites. The nanocomposites showed higher modulus values (2737–4423 MPa) compared to the pristine polymer (2693 MPa). From thermogravimetric analysis, all of the nanocomposites were stable up to 200°C and showed a two-stage degradation. © 2011 Wiley Periodicals, Inc. J Appl Polym Sci 122: 2731–2740, 2011

Key words: clay; nanocomposites; polyesters; TEM; thermogravimetric analysis (TGA)

INTRODUCTION

In recent years, polymer/layered silicate nanocomposites have attracted great interest, both in industry and in academia, because they often exhibit a remarkable improvement in materials properties compared with virgin polymers or conventional composites. These improvements can include high moduli,[1–6] increased strength and heat resistance,[7] decreased gas permeability[8–12] and flammability,[13–17] and increased biodegradability of biodegradable polymers.[18] The intercalation chemistry of appropriately modified layered silicates in polymers has been reported elsewhere.[19,20] Two major findings have stimulated the revival of interest in these materials: first, a report from the Toyota research group of a nylon 6/montmorillonite (MMT) nanocomposite,[1] for which very small amounts of layered silicate loadings resulted in pronounced improvements in the thermal and mechanical properties, and second, the observation by Vaia et al.[21] that it is possible to melt-mix polymers with layered silicates without the use of organic solvents. Today, efforts are being conducted globally with almost all types of polymer matrices.

In the field of polymer-based nanocomposites, a wide variety of materials are used as fillers, but much research has been focused on layered silicates. Two properties of layered silicates are exploitable in nanocomposite preparation; the first one is its fine particles creating a large surface area, and the second one is the ability to modify their surface chemistry.[22] The nanocomposites of thermoset polymers that can be prepared by the *in situ* intercalative polymerization method are phenol resins, epoxy resins, and unsaturated polyester resins (UPRs). Thermosets are polymers whose individual chains have been chemically linked by covalent bonds during polymerization or by subsequent chemical or thermal treatment during

Correspondence to: P. P. Kundu (ppk923@yahoo.com).

fabrication.[23] These thermosetting nanocomposites are prepared by, first, the swelling of the organically modified clay with the proper polymerazible monomers followed by crosslinking reactions

Kornmann et al.[24] reported dispersions of MMT clay in UPR that led to cured composites that displayed partial delamination of the aluminosilicate. They found that the fracture toughness doubled with the dispersion of merely 1.5 vol % aluminosilicate with concomitant increases in other mechanical properties. Suh et al.[25] demonstrated that the resulting properties of unsaturated polyester (UP) nanocomposites were greatly dependent on the preparation procedure with regard to the order of mixing of clay, polyester resin, and promoter (styrene monomer) and the curing condition. Because of the typical curing mechanism of UP, the styrene monomer, UP linear chain, and organophilically treated MMT exist together in the nanocomposite formation system. There is limited published literature on the dynamic mechanical and thermal characteristics of UP nanocomposites derived from glycolyzed poly(ethylene terephthalate) (GPET) waste.

In this research work, poly(ethylene terephthalate) (PET) waste was glycolyzed as a precursor of UPs and their nanocomposites. The product obtained was characterized by different techniques, including Fourier transform infrared (FTIR) spectroscopy, scanning electron microscopy (SEM), transmission electron microscopy (TEM), wide-angle X-ray diffraction (WAXD), dynamic mechanical analysis (DMA), and thermogravimetric analysis (TGA).

EXPERIMENTAL

Materials

Discarded PET bottles were procured from scrapers, cleaned thoroughly, and cut into small pieces (ca. 6×6 mm^2). A mixture of ethylene glycol and diethylene glycol was used for the depolymerization of PET waste with zinc acetate as a catalyst. Maleic anhydride (MA) and phthalic anhydride (PA) were used for polyesterification reactions with GPET. PA was used in the preparation of general purpose resins. For the preparation of cured resins, benzoyl peroxide was used as an initiator. These materials were obtained from CDH (New Delhi, India). The styrene monomer obtained from E. Merck (Mumbai, India) was used to reduce the viscosity of the resin and as a spacer between the crosslinks of the UP chains. All chemicals and reagents were analytical-reagent grade. MMT (K-10), with a surface area of 270 m^2/g, and dodecyltrimethylammonium bromide (DTAB), were purchased from Aldrich Chemical Co. (Milwaukee, WI). The DTAB-modified clay was used for the preparation of polyester nanocomposites.

Synthetic work

Modification of MMT

MMT clays were dispersed in deionized water by stirring. DTAB was then added to the dispersion. The whole dispersion was heated at 80°C for 6 h with vigorous stirring. A white precipitate was formed. This was isolated by filtration and washed several times with a hot 50 : 50 (v/v) water/ethanol mixture until no trace of chloride was detected in the filtrate. The treated clay was dried at 100°C in a vacuum oven for 24 h until all moisture was removed and a constant weight was obtained.

Glycolysis of PET waste

Glycolysis of PET scrap was done in a five-necked glass kettle with a mechanical agitator assembly.[26,27] The molar ratio of PET and glycol was 1 : 2. The 80 : 20 (w/w) mixture of diethylene glycol and ethylene glycol was charged in the presence of zinc acetate, a transesterification catalyst. The reactor kettle was also fitted with a reflux condenser, nitrogen inlet/outlet, and thermocouple for temperature regulation. The temperature gradually increased to 180°C, and the recycled PET flake started melting. The temperature was slowly raised by increments of 20 until a temperature of 220°C was reached. After about 5–7 h and at a cooking temperature of 230°C, all of the PET particles were visibly digested.

Synthesis of UP from GPET

UP was synthesized by the reaction of GPET with MA in the presence of *p*-toluenesulfonic acid. The relative amount of the monomers was (GPET and MA) 146 and 200 g, respectively. Because there must be a balance between diacids and glycols, the only way to control the crosslink density (ν_e) was by the introduction of different diacids or, to a lesser extent, by the use of higher molecular weight glycols. Consequently, the dilution of the maleic concentration with another diacid is generally necessary. Subsequently, MA was replaced by PA at ratios of 100 : 0, 90 : 10, 80 : 20, 70 : 30 and 60 : 40 (wt %), respectively. The temperature was maintained in the range 120–150°C for the first 5 h and then raised to 170°C for the subsequent 3 h. Water was distilled throughout the reaction. Hydroquinone (30 ppm) was added to prevent premature gelation of the resin. Then, the prepolymer was dissolved in 40 wt % styrene. It was mechanically mixed for 3 h. Constant stirring was done throughout the reaction. To initiate polymerization, 1 wt % benzoyl peroxide was added at 60°C.

Synthesis of the UP/layered silicate nanocomposites

The flowchart of the specimen preparation procedure by the *in situ* method is shown in Scheme 1. In

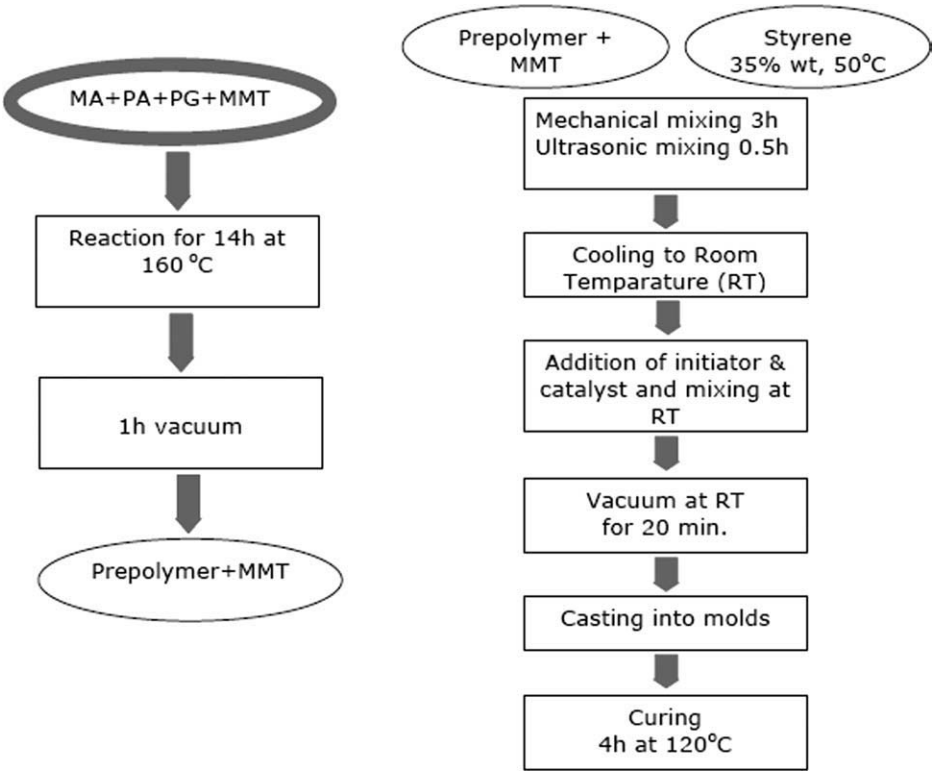

Scheme 1 Flowchart of specimen preparation by the *in situ* method.

the *in situ* method, the organoclay was added to the reaction medium simultaneously with the monomers. The penetration of the monomers into the clay layers was followed by polymerization. The nanocomposites contained 0–6 wt % organoclay with DTAB modifier. These reactants were fed together to the assembly of a five-necked glass reactor with a mechanical agitator. *p*-Toluenesulfonic acid was used as a catalyst. The whole reaction was carried out for about 8 h with constant stirring at temperatures up to 180°C. The mixture was then cooled down to 90–100°C, and hydroquinone was added to prevent premature gelation of resin. Then, the prepolymer and clay were dissolved in 40 wt % styrene. The reaction mixture was mechanically stirred for 3 h, and then, curing was done by an initiator at 1%. The initiator was thoroughly dispersed in the UP matrix in a glass vial. The materials were cured for 6 h at 60°C. The temperature was gradually increased from room temperature to 60°C at the beginning and then cooled from 60°C to room temperature at the end of the curing stage to prevent craze and cracks due to sudden crosslinking and cooling. The detailed compositions are reported in Table I. The nomenclature used in this work is based on the original composition of reactants (shown in Table I).

Characterization

FTIR spectroscopy

FTIR spectrometry with a PerkinElmer (California, USA) RX-I spectrophotometer was used to characterize the resin before and after curing. Samples were prepared by the KBr pellet method, and spectra were collected as a sum of 32 scans at a resolution of 4 cm^{-1}. Specifically, about 1 mg of finely powdered polymer sample was mixed with 100 mg of KBr powder in a mortar and pestle. The mixture was then pressed in a die at about 100 MPa of pressure for 3 min to get a transparent disk. This disk was then placed in a sample holder, and the peak transmittance was recorded.

WAXD

Scanning intensity curves for values of 2θ ranging from 4.00 to 15° were determined by X-ray diffraction (XRD) analysis (XDS 2000, Scintag, Inc.,

TABLE I
Detailed Feed Composition of the UP Nanocomposites Synthesized from GPET

Sample	Clay MMT (K^{-10}; %)	MA (%)	PA (%)	Styrene (%)
MONTUP100-4	4	100	0	40
MONTUP90-4	4	90	10	40
MONTUP80-4	4	80	20	40
MONTUP70-4	4	70	30	40
MONTUP60-4	4	60	40	40
MONTUP90-0	0	90	10	40
MONTUP90-2	2	90	10	40
MONTUP90-5	5	90	10	40
MONTUP90-6	6	90	10	40

Cupertino, CA) with powder polymeric samples. The incident X-ray beam (Cu Kα, 40 kV, 35 mA) was passed through a graphite filter and a pulse height discriminator to achieve further monochromatization.

SEM

The polymeric samples to be scanned were mounted onto the specimen stub. The samples were sputter-coated with a thin layer (ca. 25 nm) of gold under a vacuum with a sputter coater (JEOL JFM 1100, Tokyo, Japan). The coated samples were examined with a scanning electron microscope (JEOL JSM 6100) at a 25-kV accelerating voltage, and the images were recorded on 120 black-and-white roll film (100 ASA).

TEM

To prepare specimens for TEM, a small sample was microtomed with a Leica Ultracut Cryo ultramicrotome, Vienna, Austria with a Diatome diamond knife at a sample temperature of −60°C to obtain ultrathin (ca. 100–200 nm) sections. The sections were transferred onto carbon-coated Cu grids of 200 mesh. Clay layers consisting of silicon atoms appeared dark because of less electron scattering. TEM imaging was performed on a JEOL JEM 2100, Tokyo, Japan operated at a 100-kV accelerating voltage.

DMA

DMA of the bulk polymers was conducted with a PerkinElmer dynamic mechanical analyzer DMA Pyris-7e in three-point bending mode with a 110-mN static force and a 110-mN dynamic force. A rectangular specimen was prepared by the machining of the cylindrical product (obtained from heating in a vial) to specimens 1.2–2 mm in thickness and 5 mm in depth. Each specimen was first cooled under liquid nitrogen to about −30°C and then heated at 5°C/min and at a frequency of 1 Hz under nitrogen. The viscoelastic properties, that is, the storage modulus (E') and mechanical loss factor (damping; tan δ) were recorded as a function of the temperature. The glass-transition temperature (T_g) of the polymer was obtained from the peak of the loss tangent plot. The ν_e values were determined from the rubbery modulus plateau on the basis of the theory of rubber elasticity:[28,29]

$$E' = 3\nu_e RT \quad (1)$$

where E' is the storage modulus of the crosslinked polymer in the plateau region, R is the universal gas constant (8.314 J mol K), and T is the absolute temperature (K).

TGA

Thermogravimetric studies were carried out with a PerkinElmer Pyris 7 thermogravimeter under nitrogen (20 mL/min). The samples were heated from 50 to 700°C at a heating rate of 20°C/min.

RESULTS AND DISCUSSION

FTIR spectroscopy

The prepared UPR was a liquid of pale green color. At room temperature, the liquid turned to a semi-solid material. Therefore, preheating (e.g., in a water bath) was needed before it was used. FTIR was also used to observe the crosslinking of the resin. The FTIR spectra of the prepared resin before and after curing in Figure 1 showed that the result of heating (during the curing process) diminished the bands at 912 cm^{-1}, characteristic of C=C vinyl (of styrene); 981 cm^{-1}, characteristic of C—H out-of-plane bending in CHR=CHR of polyester; and 1641 cm^{-1}, indicative of the C=C of polyester. Thus, this suggested that the crosslinking occurred between polyester chains and styrene as a crosslinkable monomer at their unsaturated active sites.

WAXD

The crosslinked polyester–clay nanocomposites were studied with an X-ray diffractometer for the measurement of their crystallinity. The WAXD patterns for pure MMT [Fig. 2(a)], DTAB-modified MMT [Fig. 2(b)], and the polyester–clay nanocomposites [Fig. 2(c–f)] containing different concentrations of clay are shown in Figure 2. A strong diffraction peak at 5.47° (2θ) for MMT corresponded to a Bragg spacing (d) of the (011) plane of 15.33 Å. In Figure 2(b), a strong diffraction peak appears at 4.97° (2θ; d = 18.49 Å). When a long-chain surfactant was inserted into the hydrophilic galleries of the native clay, the interlayer distance increased, and the surface chemistry of the clay was modified (Scheme 2). The large interlayer distance suggested that the sodium ions of MMT were replaced by DTAB cations in the silicate layers.[30] The shift of peak toward a lower angle indicated intercalation of organochains inside the clay galleries. The nanocomposites prepared from the modified clays were also studied by WAXD. The peak due to MMT disappeared in the nanocomposites. This confirmed that the platy nanolayers of the clays were distorted. The vanishing of the clay peak was also observed by Su and Wilkie,[31] Riedl et al.,[32] and Davis et al.[33] According to these authors, the vanishing of the WAXD peak in the nanocomposite indicated the delamination or exfoliation of the stacked layers of the nanoclay in the polymer nanocomposites. However, Pittman et al.,[34] during their studies on the extent of the delamination of clays in polydicyclopentadiene nanocomposites, commented that the XRD results could not be

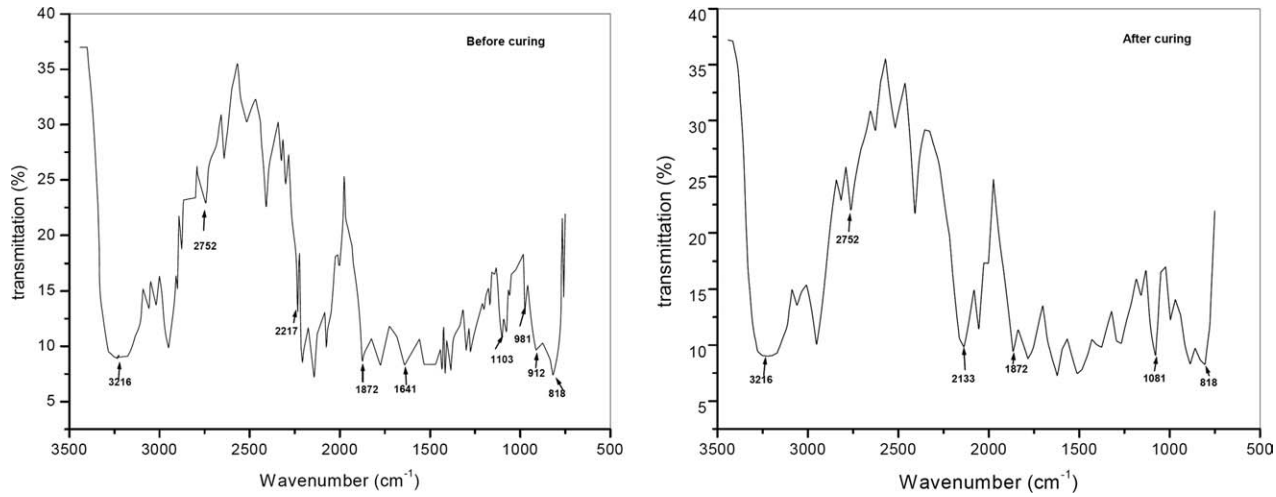

Figure 1 FTIR spectrum of the prepared UPR.

used alone as a criterion for exfoliation. Thus, although the vanishing of the peak for clays in nanocomposites (Fig. 2) apparently indicates the distortion of the nanoplaty layers, it cannot be used as a confirmatory tool. The mixing conditions (e.g., mixing time and temperature) have a significant effect on the organoclay intercalation and distortion, which was, again, influenced by the gelation time of the prepolymer.

SEM

To investigate the effect of the polymerization method and clay content on the morphological structure of the impact fractured surfaces; SEM analysis was performed. The structure of the crack propagation lines provided us with an idea about the impact strength of the material investigated. The SEM micrographs are shown in Figure 3(A–C). Figure 3(A) shows the impact surfaces of the neat UP MONTUP90-0 is a sample with 0 % MMT clay. (The details are given in Table I) at 3500×. It is obvious that the impact surface was smooth, and few straight crack propagation lines were observed; this explains the low impact strength of this material. Figures 3(B) (MONTUP90-4) and 3(C) (MONTUP90-5) show the impact surfaces of the nanocomposites at the same magnification prepared by the *in situ* methods. In Figure 3(B), it is observed that the crack propagation lines approached a shorter and closer structure at 4% clay loading; this means that the crack propagation path was tortuous and prevented the easy propagation of cracks. This resulted in a higher impact strength in the samples prepared by the *in situ* method. In Figure 3(B), the crack propagation lines also have a shorter and closer structure in comparison to that in Figure 3(A); this shows the SEM micrograph of neat UP. However, with the addition of 5 wt % organoclay, the decrease in the impact strength could be attributed to the agglomeration of the clay particles [Fig. 3(C)], which acted as stress concentrators at higher clay loadings.

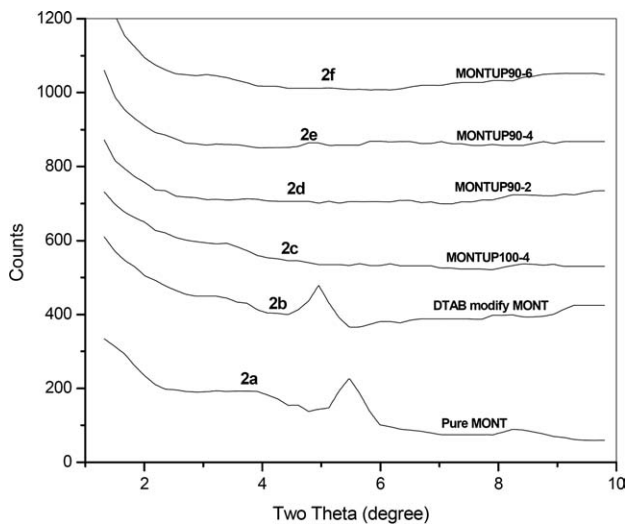

Figure 2 WAXD pattern for (a) pure clay, (b) modified clay, and (c–f) polymer nanocomposites with various clay and unsaturated acid contents.

TEM

More direct evidence for the formation of a nanocomposite was provided by TEM of an ultramicrotomed

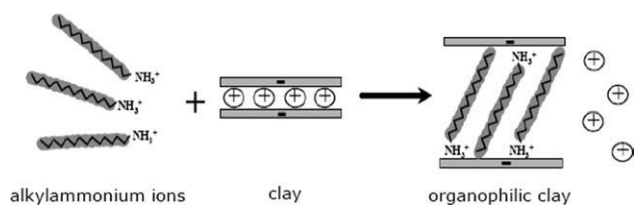

Scheme 2 Cation-exchange process between alkyl ammonium ions and cations initially intercalated between the clay layers.

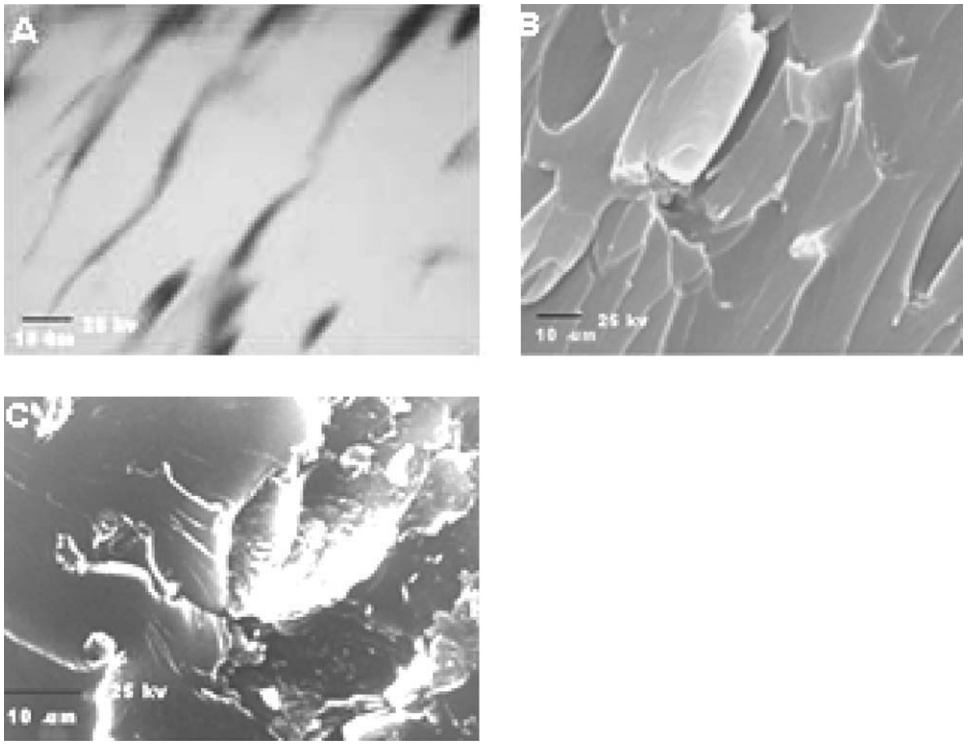

Figure 3 SEM micrographs at the magnification of 3500× and a scale of 10 μm for (A) neat UP, (B) UP nanocomposite at 4% clay loading, and (C) UP nanocomposite at 5% clay loading.

section. The TEM images in Figures 4 and 5 display individual silicate layers (which appear as dark lines). There were some irregular dispersions of the silicate layer. Some particles of the silicate layers maintained their original ordering, whereas some were exfoliated. The TEM micrographs are shown in Figures 4

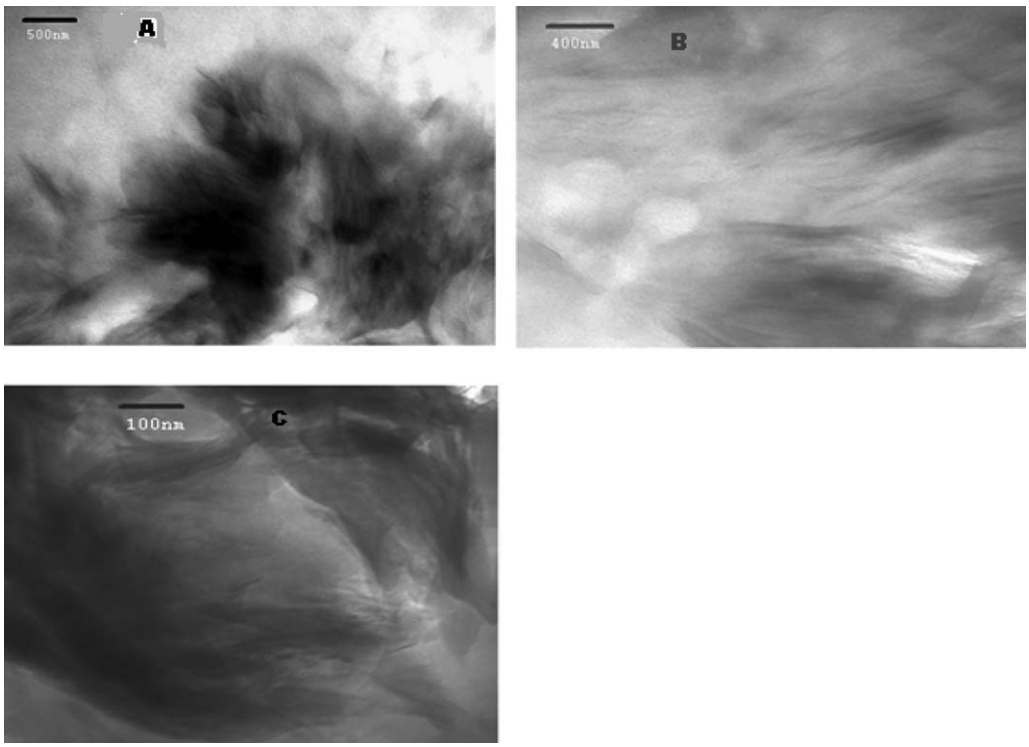

Figure 4 TEM images of UP nanocomposite containing 2 wt % clay: (A) low magnification and (B) intercalated and exfoliated sheets at high magnification of the aggregate region shown in the exfoliated sheets from parts A and C.

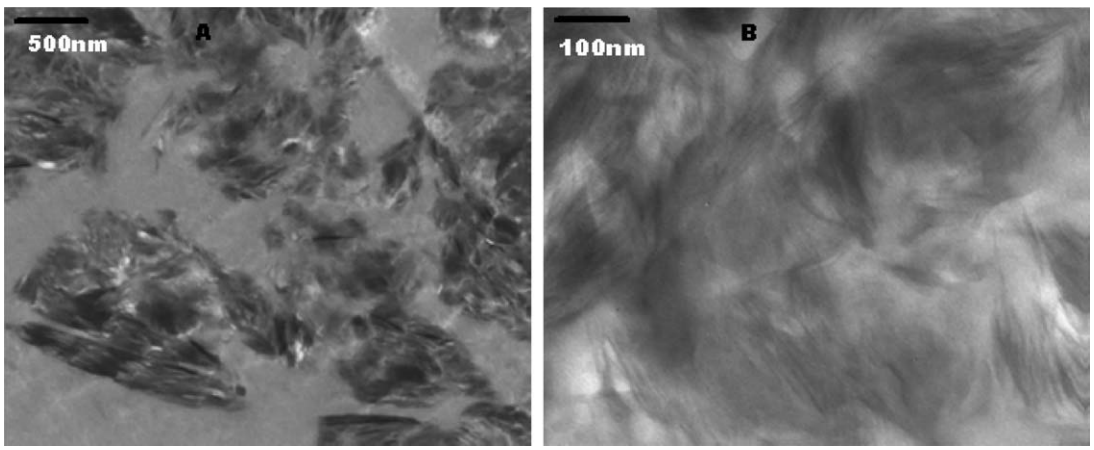

Figure 5 TEM images of the UP nanocomposite containing 4 wt % clay: (A) low and (B) high magnifications. Both the intercalated and exfoliated regions were investigated.

(MONTUP90-2) and 5 (MONTUP90-4) at different magnifications. The dispersion of micrometer-sized aggregates in the matrix at low magnification are shown in Figures 4(A) and 5(A). Fewer aggregates are shown in Figure 4(A). As evident from Figures 4(B) and 5(B) at higher magnification, individual sheets of clay were clearly separated by a layer of polymer. From Figure 4(C), individual dispersion of the completely delaminated sheets in the matrix were observed. Hence, it could be concluded that the morphology of the crosslinked polyester–clay nanocomposite could be described as a dispersion of intercalated and exfoliated aggregates in the matrix.

Viscoelastic properties

Figure 6 shows the plots of E' and tan δ against temperature for different nanocomposite samples. In all of the E' curves, we observed that the modulus decreased continuously with an increase in temperature. Figure 6(a) shows the E' plots for the GPET-based UP nanocomposites with different unsaturated acid contents (60–100%) with the concentration of clay kept fixed at 4 wt %. It was observed that E' increased with an increase in the unsaturated acid content (weight percentage) in the polyester nanocomposites. Five different weight percentages of the unsaturated acid were used in the synthesis of these nanocomposites with 4% modified clay. As observed from Figure 6(a) and Table II, the increase in the unsaturated acid content resulted in increases in E' and T_g of the samples. It is well known that during polyesterification of MA at high temperature, a part of maleic (cis) unsaturation isomerizes into fumarate (trans) form.[35] The extent of isomerization is a function of the temperature and unsaturated content of the polyesterification reaction.[36] The isomerization has a profound effect on the mechanical properties of the UPs.[37] The fumaric double bond reacts more readily with styrene than the maleic double bond, thereby providing a higher ν_e than the corresponding maleic unsaturation. It is noteworthy that the

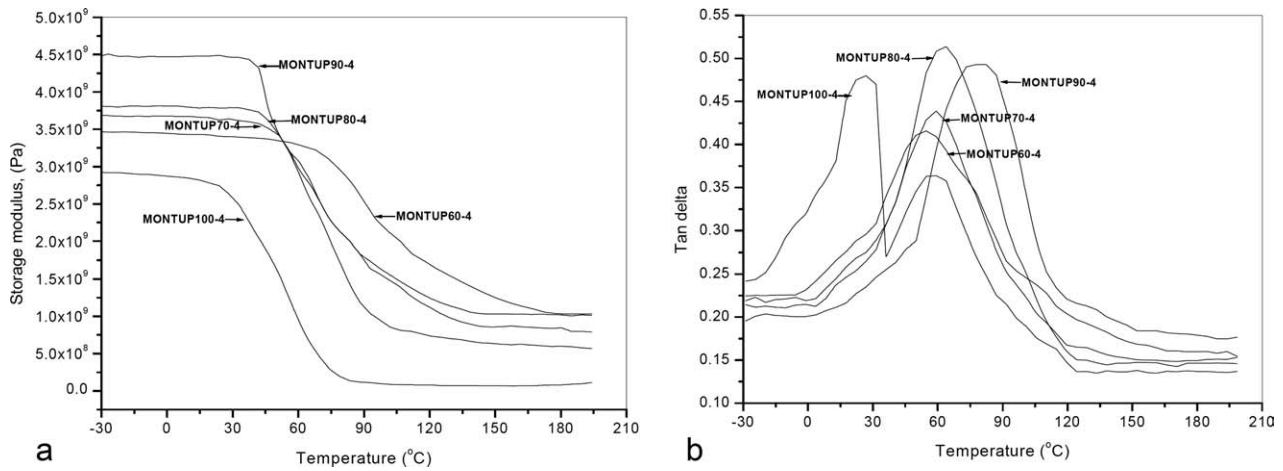

Figure 6 Temperature dependence of (a) E' and (b) tan δ of UP nanocomposites with different unsaturated acid contents (60–100%) with the clay fixed at 4 wt %.

TABLE II
T_g, E', and ν_e for Different UP Nanocomposite Samples from DMA

Sample	T_g (°C)	E' (MPa)	$\nu_e \times 10^5$ (mol/m^3)
MONTUP100-4	34.00, 58.00	2737	3.70
MONTUP90-4	78.21	4423	5.72
MONTUP80-4	63.12	3740	4.76
MONTUP70-4	58.85	3584	4.57
MONTUP60-4	54.57	3240	4.02
MONTUP90-0	54.00	2693	3.52
MONTUP90-2	65.00	3792	4.76
MONTUP90-5	54.20	3651	4.60
MONTUP90-6	50.00	3469	4.29

sample with 100% unsaturated acid content showed a modulus even lower than the sample with 60% unsaturated acid content and also showed two glass-transition peaks [Fig. 6(b)]. This indicates that there was phase separation in the sample with 100% unsaturated acid content, due to which the soft segment showed a lower transition temperature (34°C) and the hard segment showed a higher T_g (58°C). Because the dilution of maleic concentration with another diacid was necessary to control ν_e, in the case of sample with 100% unsaturated acid content, there was an imbalance between diacid and glycol. This led to phase separation and a lower modulus value (also evident from the lower ν_e). The hard segment, which contained mainly the crosslinking part of styrene and unsaturated acid, showed T_g at a higher temperature. In Table II, it is shown that the modulus and ν_e followed up sequence with respect to the unsaturated acid content. This was because the modulus of the nanocomposite samples was observed to increase with an increase in the unsaturated acid content. With the increase in clay content from 0 to 4%, there was an increase in the modulus and ν_e. The decrease in modulus and ν_e may have been due to the tendency of clay particles to agglomerate due to poor dispersion at high clay contents.

In Figure 7, E' and tan δ are plotted against temperature for polyester samples with 0–6% modified MMT clay at a fixed composition. It is shown in the E' curve [Fig. 7(a)] that the pristine polymer showed the lowest modulus compared with all of the other nanocomposite samples. This was due to mixing of the modified clay particles in the polymer matrix at the molecular level. Also, the blending effects of the clay surface on the motion of matrix molecular chains and the friction between them increased. However, in all of the nanocomposite samples, the sample with 6% clay showed the lowest E'. This was due to the aggregation of the nanoclay particles in the polymer matrix at a higher concentration (6%), because of which the nanofiller behaved just like an ordinary filler. The sample with 4% nanofiller showed the highest modulus, and the modulus increased with increasing nanofiller content. It was observed during the swelling studies of these samples that the sample with 4% nanofiller had the finest barrier properties. Thus, the nanocomposite behavior was observed to be the best at a 4% level of nanofiller.

From Figure 7(b), the T_g values of the samples with different clay contents at the same polymer composition were determined from the maxima of tan δ. It is evident from Table II and Figure 7(b) that T_g increased from 54 to 78.21°C with the addition of 0–4 wt % nanofiller. This tan δ primarily represents the ratio of the dissipation energy to the energy stored in the specimen during the applied alternating strain cycle. The shift of the tan δ peak to a higher temperature indicated an increase in T_g of the nanocomposites. Because the glass-transition process is related to the molecular motion, T_g is considered to be affected by molecular packing, chain rigidity, and linearity.[38] The increase in T_g of all of the nanocomposite samples in comparison with the pristine

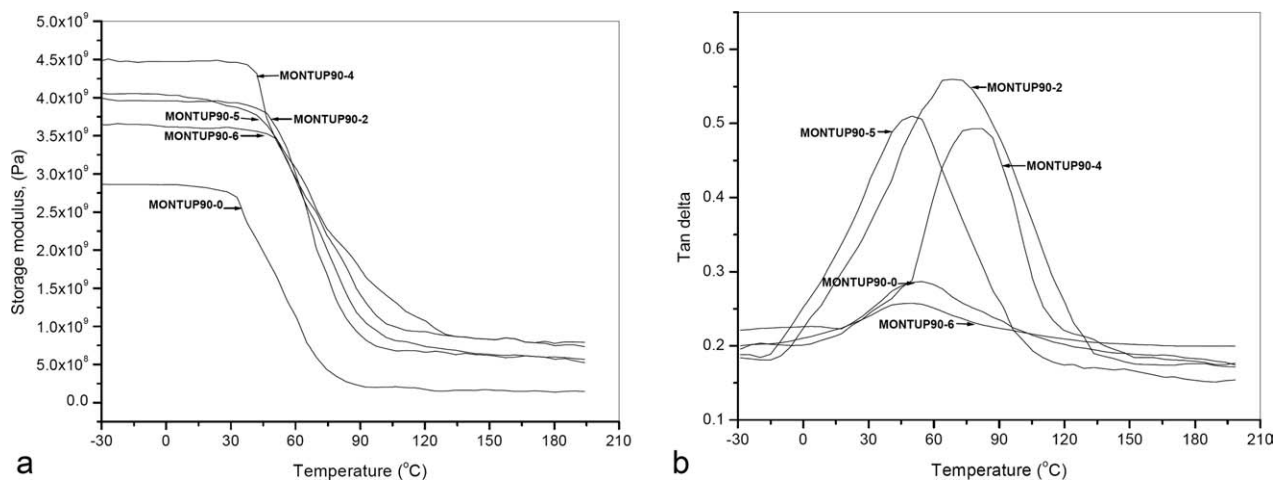

Figure 7 Temperature dependence of (a) E' and (b) tan δ of UP nanocomposites with different clay contents (0–6%) and the same polymer composition.

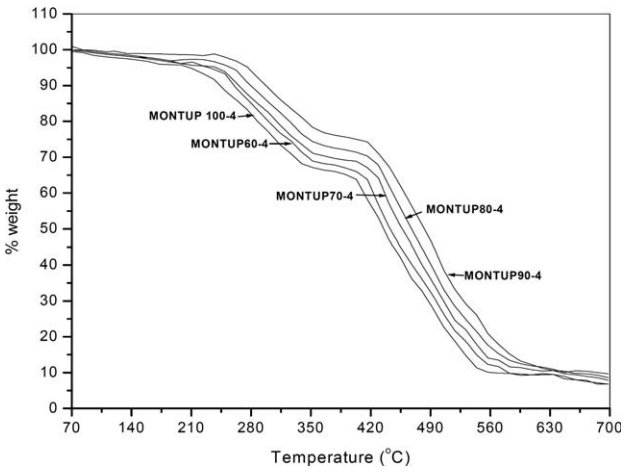

Figure 8 TGA curves of the UP nanocomposites with different unsaturated acid contents (60–100%) with the clay fixed at 4 wt %.

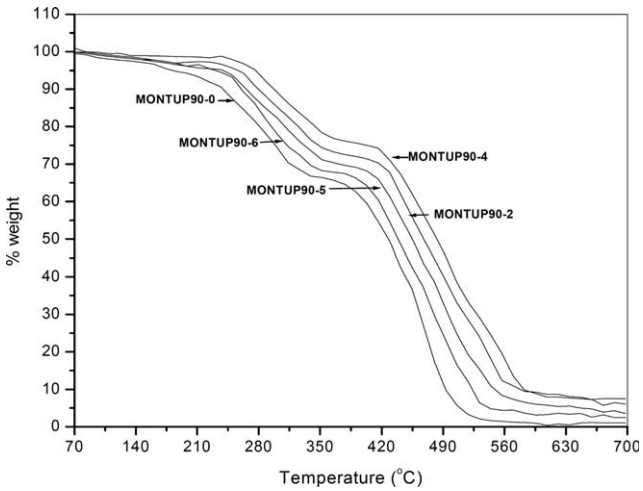

Figure 9 TGA curves of the UP nanocomposites with different clay contents (0–6%) and the same polymer composition.

polymer could be attributed to the mixing at the nanolevel of the filler; this, thereby, increased the content of hard segment in the polymer matrix.[39] Such increases in T_g on the order of few degrees were more specifically attributed to restricted relaxation near the interface of the inorganic–organic nanocomposites. The details of the dynamic mechanical properties are reported in Table II.

Thermal analysis

One of the most important property enhancements expected upon formation of a polymer nanocomposite is the retardation of thermal degradation.[40,41] Figures 8 and 9 show the TGA curves for different polyester samples in a nitrogen atmosphere. Both figures indicate degradation in two stages for all of the samples. The first and second stages were observed between 250 and 410°C and between 410 and 560°C, respectively. The first stage was due to the evaporation of the uncrosslinked portion, and the second stage was due to the degradation of the crosslinked networks in the polymer nanocomposites. Table III illustrates the TGA results for the GPET waste nanocomposites. T_5, T_{10}, and T_{50} represent the temperatures at which the 5, 10, and 50% weight losses occurred. T_5 and T_{10} are in the first stage and are generally used to evaluate the thermal stability of the bulk polymer.[42,43] T_{50} is in the second stage and reflects the consistency of the crosslinked networks of the bulk polymer. The onset of degradation temperature (at 5% weight loss) was above 250°C, which is higher than that for the pristine polymer. In all of the nanocomposite samples, about 7% residue was left at the end of the experiment (to a temperature of 700°C). The leftover mass was due to the clay in the nanocomposite, which was quite stable.[44] All of the curves became flat, and mainly, the inorganic residue (i.e., Al_2O_3, MgO, SiO_2) remained at the end. As shown in Figure 8, all of the samples showed an onset of degradation above 250°C, except for the sample containing 100% unsaturated acid contents. This anomalous behavior was due to a molar excess of the unsaturated dicarboxylic acid, whose reactive double bonds were distributed much more densely, and the reactivity was higher, as there was a larger number of reactive sites in each polyester chain. This also provided a much denser network in the cured resin, which resulted in a brittle material with poor thermal and mechanical properties. The first-stage degradation started around 200°C and continued up to 400°C. The second stage started at 400°C and continued up to 550°C. The details of T_5, T_{10}, and T_{50} are reported in Table III. It was observed that the degradation temperature increased with an increase in the unsaturated content. The reactivity of the acid increased because of the presence of clay, which was a mixture of different metal ions, such as Na^+, K^+, Al^{3+}, and Mg^{2+}. These metal ions acted as a catalyst for the unsaturated acid polymerization. The sample with 90% unsaturated acid content showed better stability

TABLE III
Degradation Results from TGA Experiments for Different Polyester Nanocomposites

Sample	T_5 (°C)	T_{10} (°C)	T_{50} (°C)
MONTUP100-4	206	242	435
MONTUP90-4	273	261	440
MONTUP80-4	247	265	452
MONTUP70-4	232	274	464
MONTUP60-4	230	295	482
MONTUP90-0	181	237	427
MONTUP90-2	248	277	469
MONTUP90-5	234	262	456
MONTUP90-6	231	258	437

than other samples. This indicated that this sample was superior to the others as the stability of the sample was higher. The presence of more double bonds in the unsaturated polymer enhanced the rate of curing and led to the formation of tightly bound nanocomposites. This caused higher stability.

Figure 9 shows the TGA curves for the polymer nanocomposites with various clay contents (0–6%) and the same polymer feed composition. The onset of degradation was slightly but progressively hastened upon addition of clay compared to the pure polymer. The pure polymer was completely decomposed at 500°C. It was also observed that the sample with 4% clay showed better stability between 350 and 410°C. It was not surprising that the nanocomposites showed slower degradation above 600°C because there was only inorganic aluminosilicate left in the system at that stage. In whole, all of the nanocomposite samples had similar degradation patterns. TGA indicated that the polymer resins obtained after the recycling of PET bottles had a high thermal resistance and could be used in various civil engineering applications as a binder.

CONCLUSIONS

Nanocomposites from GPET, with varied compositions of PA and MA, were successfully synthesized with modified MMT clay. The nanoclay remarkably improved the properties of the PET waste UP. The peaks observed in modified MMT in the WAXD graph vanished completely in the nanocomposites; this indicated the complete distortion of platy nanolayers of the nanoclay in the nanocomposites. Thermal and mechanical characterization of the MMT-filled nanocomposites helped to establish criteria for the selection of materials for specific use. It was observed that with an increase in unsaturated acid content at a fixed nanoclay loading, the value of E' varied from 2737 to 4423 MPa. The T_g's measured through DMA ranged from 54.57 to 78°C, and ν_e ranged from 3.70×10^5 to 5.72×10^5 mol/m^3. The DMA results showed an enhanced E' and transition temperature compared with the pristine polymer. It was confirmed by TGA that unlike pristine polymer, all samples were stable up to 200°C and showed a two-stage degradation. The first stage was observed between 250 and 410°C, and the second stage was observed between 410 and 560°C.

References

1. Okada, A.; Kawasumi, M.; Usuki, A.; Kojima, Y.; Kurauchi, T.; Kamigaito, O. In Polymer Based Molecular Composites; Schaefer, D. W., Mark, J. E., Eds.; MRS Symposium Proceedings; Pittsburgh: 1990; Vol. 171, p 45.
2. Giannelis, E. P. Adv Mater 1996, 8, 29.
3. Giannelis, E. P.; Krishnamoorti, R.; Manias, E. Adv Polym Sci 1999, 138, 107.
4. Lebaron, P. C.; Wang, Z.; Pinnavaia, T. J. Appl Clay Sci 1999, 15, 11.
5. Vaia, R. A.; Price, G.; Ruth, P. N.; Nguyen, H. T.; Lichtenhan, J. Appl Clay Sci 1999, 15, 67.
6. Biswas, M.; Sinha, R. S. Adv Polym Sci 2001, 155, 167.
7. Giannelis, E. P. Appl Organomet Chem 1998, 12, 675.
8. Xu, R.; Manias, E.; Snyder, A. J.; Runt, J. Macromolecules 2001, 34, 337.
9. Bharadwaj, R. K. Macromolecules 2001, 34, 1989.
10. Messersmith, P. B.; Giannelis, E. P. J Polym Sci Part A: Polym Chem 1995, 33, 1047.
11. Yano, K.; Usuki, A.; Okada, A.; Kurauchi, T.; Kamigaito, O. J Polym Sci Part A: Polym Chem 1993, 31, 2493.
12. Kojima, Y.; Usuki, A.; Kawasumi, M.; Fukushima, Y.; Okada, A.; Kurauchi, T.; Kamigaito, O. J Mater Res 1993, 8, 1179.
13. Gilman, J. W.; Kashiwagi, T.; Lichtenhan, J. D. SAMPE J 1997, 33, 40.
14. Gilman, J. W. Appl Clay Sci 1999, 15, 31.
15. Dabrowski, F.; Bras, M. L.; Bourbigot, S.; Gilman, J. W.; Kashiwagi, T. Presented at the Eurofillers 99, Lyon-Villeurbanne, France, Sept 1999.
16. Bourbigot, S.; Lebras, M.; Dabrowski, F.; Gilman, J. W.; Kashiwagi, T. Fire Mater 2000, 24, 201.
17. Gilman, J. W.; Jackson, C. L.; Morgan, A. B.; Manias, E.; Giannelis, E. P.; Wuthenow, M.; Hilton, D.; Phillips, S. H. Chem Mater 2000, 12, 1866.
18. Sinha, R. S.; Yamada, K.; Okamoto, M.; Ueda, K. Nano-Lett 2002, 2, 1093.
19. Blumstein, A. J Polym Sci Part A: Gen Pap 1965, 3, 2665.
20. Theng, B. K. Formation and Properties of Clay–Polymer Complexes; Elsevier: Amsterdam, 1979.
21. Vaia, R. A.; Ishii, H.; Giannelis, E. P. Chem Mater 1993, 5, 1694.
22. Rothon, R. N. Particulate-Filled Polymer Composites, 2nd ed.; Rapra Technology: Shropshire, England, 2003.
23. Fried, J. R. Polymer Science and Technology; Prentice Hall: Upper Saddle River, NJ, 1995.
24. Kommann, X.; Berglund, L. A.; Sterete, J.; Giannelis, E P. Polym Eng Sci 1998, 38, 1351.
25. Suh, D. J.; Lim, Y. T.; Park, O. O. Polymer 2000, 41, 8557.
26. Vaidya, U. R.; Nadkarni V. M. Ind Eng Chem Res 1987, 26, 194.
27. Vaidya, U. R.; Nadkarni V. M. J Appl Polym Sci 1987, 34, 235.
28. Li, F.; Larock, R. C. Biomacromolecules 2003, 4, 1018.
29. Kundu, P. P.; Larock, R. C. Biomacromolecules 2005, 6/2, 797.
30. Ou, C. F.; Ho, M. T.; Lin, J. R. J Polym Res 2003, 10, 127.
31. Su, S.; Wilkie, C. A. J Polym Sci Part A: Polym Chem 2003, 41, 1124.
32. Feng, W.; Ait-Kadi, A.; Riedl, B. Macromol Rapid Commun 2002, 23, 703.
33. Davis, C. H.; Mathias, L. J.; Gilman, J. W.; Schiraldi, D. A.; Shields, J. R.; Trulove, P.; Sutto, T. E.; Delong, H. C. J Polym Sci Part B: Polym Phys 2002, 40, 2661.
34. Yoonessi, M.; Toghiani, H.; Kingery, W. L.; Pittman, C. U., Jr. Macromolecules 2004, 37, 2511.
35. Vaidya, U. R.; Nadkarni V. M. Ind Eng Chem Res 1988, 27, 2056.
36. Vancso Szmercsanyi, I.; Maros Greger, K.; Makay Bodi, E. J Polym Sci 1961, 53, 241.
37. Boenig, H. V. In Encyclopedia of Polymer Science and Technology; Wiley: New York, 1969; Vol. 11, p 129.
38. Kandary, A. I.; Ali, A. M.; Ahmad, Z. J Appl Polym Sci 2005, 98, 2521.
39. Li, F.; Ge, J. J.; Honigfort, P. S.; Harris, F. W. Polymer 1999, 40, 4987.
40. Sur, G. S.; Sun, H. L.; Lyu, S. G.; Mark, J. E. Polymer 2001, 42, 9783.
41. Bandyopadhyay, S.; Giannelis, E. P. Polym Mater Sci Eng 2000, 82, 208.
42. Li, F.; Larock, R. C. J Appl Polym Sci 2001, 80, 658.
43. Li, F.; Hasjim, J.; Larock, R. C. J Appl Polym Sci 2003, 90, 1830.
44. Marras, S. I.; Tsimpliaraki, A.; Zuburtikudis, I.; Panayiotou, C. J. Colloid Interface Sci 2007, 315, 520.